Acta Biochimica Polonica

Vol. 54 No. 3/2007, 509–522

on-line at: www.actabp.pl

Regular paper

The DnaK chaperones from the archaeon *Methanosarcina mazei* and the bacterium *Escherichia coli* have different substrate specificities

Michal A. Żmijewski[1★], Joanna Skórko-Glonek[1], Fabio Tanfani[2], Bogdan Banecki[3], Agnieszka Kotlarz[1], Alberto J.L. Macario[4]✉ and Barbara Lipińska[1]✉

[1]Department of Biochemistry, University of Gdańsk, Gdańsk, Poland; [2]Institute of Biochemistry, Faculty of Sciences, Universita Politecnica delle Marche, Ancona, Italy; [3]Department of Molecular and Cellular Biology, Faculty of Biotechnology, University of Gdańsk, Gdańsk, Poland; [4]Center of Marine Biotechnology, University of Maryland Biotechnology Institute, Baltimore, Maryland, USA

Received: 28 June, 2007; revised: 06 September, 2007; accepted: 12 September, 2007
available on-line: 17 September, 2007

Hsp70 (DnaK) is a highly conserved molecular chaperone present in bacteria, eukaryotes, and some archaea. In a previous work we demonstrated that DnaK from the archaeon *Methanosarcina mazei* ($DnaK_{Mm}$) and the DnaK from the bacterium *Escherichia coli* ($DnaK_{Ec}$) were functionally similar when assayed *in vitro* but $DnaK_{Mm}$ failed to substitute for $DnaK_{Ec}$ *in vivo*. Searching for the molecular basis of the observed DnaK species specificity we compared substrate binding by $DnaK_{Mm}$ and $DnaK_{Ec}$. $DnaK_{Mm}$ showed a lower affinity for the model peptide (a-CALLQSRLLS) compared to $DnaK_{Ec}$. Furthermore, it was unable to negatively regulate the *E. coli* σ^{32} transcription factor level under heat shock conditions and poorly bound purified σ^{32}, which is a native substrate of $DnaK_{Ec}$. These observations taken together indicate differences in substrate specificity of archaeal and bacterial DnaKs. Structural modeling of $DnaK_{Mm}$ showed some structural differences in the substrate-binding domains of $DnaK_{Mm}$ and $DnaK_{Ec}$, which may be responsible, at least partially, for the differences in peptide binding. Size-exclusion chromatography and native gel electrophoresis revealed that $DnaK_{Mm}$ was found preferably in high molecular mass oligomeric forms, contrary to $DnaK_{Ec}$. Oligomers of $DnaK_{Mm}$ could be dissociated in the presence of ATP and a substrate (peptide) but not ADP, which may suggest that monomer is the active form of $DnaK_{Mm}$.

Keywords: archaeal Hsp70(DnaK), substrate-binding by archaeal DnaK, archaeal DnaK quaternary structure

INTRODUCTION

The Hsp70 proteins form a family of evolutionarily conserved heat shock proteins which act as molecular chaperones, assisting in the folding of nascent polypeptides, in the refolding of partially denatured proteins and in many other cellular processes. They have a weak ATPase activity and function by reversibly binding substrates at the expense of ATP hydrolysis. The Hsp70s of prokaryotic organisms are called the DnaK proteins, after the model protein of *Escherichia coli,* and function as a triad, together with the co-chaperones Hsp40 (DnaJ) and GrpE (Bukau *et al*., 2000; 2006; Truscott *et al.,* 2003;

✉**Corresponding authors**: Barbara Lipińska, Department of Biochemistry, University of Gdańsk, Kładki 24, 80-822 Gdańsk, Poland; tel. (48 58) 305 9278; fax (48 58) 301 5741; e-mail: lipinska@biotech.ug.gda.pl; Alberto J.L. Macario, Center of Marine Biotechnology, University of Maryland Biotechnology Institute, 701 E. Pratt Str., Baltimore, Maryland 21202, USA; tel.: 410-234-8849; fax: 410-234-8896; e-mail: macario@umbi.umd.edu

★Present address: Department of Pathology and Laboratory Medicine, University of Tennessee Health Science Center, 19S Manassas Ave., Memphis, Tennessee 38163, USA.

Abbreviations: a-p4, acrylodan labeled peptide (a-CALLQSRLLS); $DnaJ_{Ec}$, DnaJ protein of *E. coli*; $DnaJ_{Mm}$, DnaJ protein of *M. mazei*; $DnaK_{Ec}$, DnaK protein of *E. coli*; $DnaK_{Mm}$, DnaK protein of *M. mazei*; FT-IR, Fourier-transform infrared; NR peptide, DnaK substrate (NRLLLTG); SBD, substrate-binding domain of DnaK protein; SPR, surface plasmon resonance spectroscopy.

Deuerling & Bukau 2004; Young *et al.,* 2004; Kultz 2005).

DnaK of *E. coli* is composed of two domains: an approximately 44 kDa amino-terminal ATPase domain and a carboxy-terminal substrate binding domain (SBD) of about 27 kDa. The crystal structures of the ATPase domain (Harrison *et al.*, 1997) and that of the SBD (Zhu *et al.,* 1996) have been solved. The ATPase domain contains a groove for ATP binding; it also binds a dimeric form of the nucleotide-exchange factor GrpE. In the structure of SBD two subdomains exist: the first one, composed mostly of β-sheets, containing a cavity which binds the substrate polypeptide (displaying short stretches of hydrophobic residues on its surface), and the second one, composed mostly of α-helices, which functions as a lid covering the peptide-binding cavity (Zhu *et al.*, 1996).

According to the current model, the α-helical subdomain forming a latch over the substrate-binding cavity is in an open conformation in the ATP-bound state, allowing release of the folded polypeptide and subsequent binding of another molecule of substrate to initiate a second folding cycle. The capture and retention of the polypeptide for folding involves closing of the latch, a conformational change that requires energy from the hydrolysis of the bound ATP, which is converted to ADP. Since the ADP-bound DnaK has a higher affinity for the peptide compared to the ATP-bound form, in order to release the polypeptide, ADP has to be exchanged for ATP. Both the ATPase activity of DnaK and nucleotide exchange are regulated by the co-chaperones DnaJ and GrpE. The amino-terminal DnaJ domain binds to DnaK and stimulates ATP hydrolysis, which promotes substrate binding. Subsequently, GrpE promotes ADP dissociation thus enabling DnaK to bind ATP, which in turn promotes the DnaK-polypeptide complex dissociation and release of the folded polypeptide (Bukau *et al.*, 2000; 2006; Mayer *et al.,* 2000; Deuerling & Bukau, 2004; Erbse *et al.*, 2004; Young *et al.,* 2004).

In *E. coli*, the *dnaK, dnaJ* and *grpE* genes belong to a heat shock regulon positively controlled by the *rpoH* gene product, a promoter-specific σ^{32} subunit of RNA polymerase. DnaK negatively regulates the level of σ^{32} by binding and promoting its proteolysis (Yura & Nakahigashi, 1999). The binding of σ^{32} by DnaK is an example showing that not only unfolded polypeptides but also a native, non-denatured protein may be a substrate for this chaperone (Liberek *et al.*, 1992).

The Hsp70/DnaK proteins are highly conserved in sequence and distribution in Bacteria and Eukarya, but in the Archaea DnaK is present only in some species, one of which is a mesophilic archaeon, *Methanosarcina mazei* (Macario *et al.,* 1991). It is hypothesized that the archaeal DnaK system has been obtained by lateral transfer of the *dnaK-dnaJ-grpE* genes from bacteria. This hypothesis is well documented, mainly on the basis of sequence similarity (Gribaldo *et al.*, 1999; Macario & Conway De Macario, 2001; Macario *et al.*, 2004) and, recently, by showing a functional and structural similarity of purified *M. mazei* and *E. coli* DnaK proteins (Żmijewski *et al.,* 2004; 2007). These similarities notwithstanding, there is a significant functional difference, revealed by the fact that the *dnaK* gene of *M. mazei* is unable to complement *dnaK* mutations in *E. coli*. *E. coli dnaK* mutant bacteria are thermosensitive and this phenotype can not be rescued by DnaK of *M. mazei* (Żmijewski *et al.,* 2004), which indicates DnaK species-specificity.

Generally, chaperones are considered to be promiscuous, since *in vitro* they interact with a variety of unfolded polypeptides and the presence of exposed hydrophobic groups seems to be the only requirement for Hsp70 binding (Erbse *et al.*, 2004). However, DnaK from one species introduced into another is frequently unable to fully substitute for the DnaK of the host cell (Sussman & Setlow, 1987; Mehlert & Young, 1989; Tilly *et al.,* 1993; Minder *et al.,* 1996; Mogk *et al.,* 1999). Since the species-specificity of DnaK proteins is an unsolved problem and because very little is known so far about function of the archaeal DnaKs, we decided to investigate molecular basis of the observed species-specificity of the *M. mazei* DnaK.

In this work we compared the binding of a typical peptide substrate, representing an unfolded protein, and of a native protein, sigma 32 transcription factor, by $DnaK_{Mm}$ and $DnaK_{Ec}$. Searching for structural differences we analyzed the oligomerization status of the purified DnaKs. Our results showed a significantly lower affinity of the $DnaK_{Mm}$ for both types of substrates, and also differences in the quaternary structures of the purified DnaKs.

MATERIALS AND METHODS

Bacterial strains, plasmids, media. The *Escherichia coli* strains and plasmids used in this study are listed in Table 1. LB medium (Luria-Bertani broth) and LA (Luria agar) were prepared according to Sambrook and coauthors (1989), and were supplemented with appropriate antibiotics (when necessary): 100 μg ml^{-1} ampicillin, 68 μg ml^{-1} chloramphenicol, and 30 μg ml^{-1} kanamycin.

Chemicals. Deuterium oxide (99.9% ^2H_2O), ^2HCl, and NaO^2H were purchased from Aldrich (Sigma-Aldrich S.r.l., Milan, Italy). All other chemicals were commercial products of the purest quality

Table 1. ***Escherichia coli*** **strains and plasmids used in this study.**

E. coli strain or plasmid---Relevant genotype	Source/Reference
B178---W3110 *galE sup*$^+$	BDUG collection[a]
MC4100---F$^-$ *araD* Δ(*argF-lac*)*U169 rpsL relA flbB deoC ptsF rbsR*	BDUG collection
BM271--- MC4100 Δ*dnaK*52::Cm^R*ts*	B. Bukau/(Paek & Walker, 1987)
CG50---B178 *dnaK*756*ts*	C. Georgopoulos/(Sell *et al.*, 1990)
DA259---C600 Δ*grpE*::Ω-Cm^R *thr*::Tn*10*	D. Ang/(Wu *et al.*, 1994)
Plasmids	
pMOB45-$dnaK_{Ec}$---pMOB45-$dnaK_{Ec}$ Cm^R	BDUG collection/(Zylicz & Georgopoulos, 1984)
pJZ-589---pTTQ19-*ptac*$dnaK_{E.\ coli}$ $dnaJ_{E.\ coli}$ Amp^R	D. Wall *via* S. Kedzierska/(Kedzierska *et al.*, 1999)
pAM1---PBS–$dnaK_{Mm}$ Amp^R	A.J.L. Macario/R. Kim
pAM4---PBS–$dnaKJ_{Mm}$ Amp^R	A.J.L. Macario/R. Kim
pBS---PBS (pBlueScript) Amp^R	BDUG collection/Stratagene
pAK1---pT7-5-*rpoH* Amp^R	BDUG collection/(Kotlarz *et al.*, 1998)
pGP1-2---T7pol Kan^R	BDUG collection/(Tabor & Richardson, 1985)

[a]BDUG, Biochemistry Department, University of Gdańsk

purchased from Sigma (Poznań, Poland), or were obtained as indicated in the text.

Proteins, peptides, electrophoresis, and immunoblotting. DnaK proteins from *M. mazei* and *E. coli* were purified as described previously (Żmijewski *et al.*, 2004). The proteins were dialyzed against 25 mM Hepes, 100 mM KCl, 10% glycerol, pH 7.2. Protein (>95% pure) concentrations were determined by the Bradford method (Bradford, 1976) and were confirmed by densitometry of Coomassie-stained sodium dodecyl sulphate polyacrylamide-gel electrophoresis (SDS/PAGE) gels, using BSA as a standard protein. DnaK preparations were free of ATP, as tested by the malachite green method (Lanzetta *et al.*, 1979) as we described before (Żmijewski *et al.*, 2004). Sigma 32 (σ^{32}) protein was prepared as described (Kotlarz *et al.*, 1998). Acrylodan (6-acryloyl-2-dimethylaminonaphthalene) labeled peptide a-p4 (a-CALLQSRLLS), prepared as described (Gisler *et al.*, 1998), was a generous gift of Professor J. P. Christen (Zurich, Switzerland). NR peptide (NRLLLTG) of at least 95% purity was purchased from GenoMed (GenoMed, Inc., St. Louis, MO, USA). Peptides were stored in 30% (v/v) acetonitrile at 100 μM concentration, at –70 °C. Proteins were analysed by SDS/PAGE according to Laemmli (1970), using 10 or 12.5% (w/v) acrylamide. Native gel electrophoresis was performed using the Laemmli system without SDS and without stacking gel, in 10% resolving gels. Before the native electrophoresis, proteins (3 μM) were incubated for 30 min in 50 mM Hepes, pH 7.5, 50 mM KCl, and 10 mM $MgCl_2$ buffer, in the presence of either 3 mM ATP or 3 mM ADP+Pi, or in the absence of nucleotide; or in the presence of 200 nM peptide NR (NRLLLTG) as indicated in figure legends. Immunoblotting was performed as described before (Żmijewski *et al.*, 2004), using anti-σ^{32} polyclonal rabbit antibodies raised by immunization with purified σ^{32} protein (Szewczyk & Harper, 1994).

Protein modeling. Modeling of *M. mazei* chaperone proteins was done by use of the Swiss Model server and Deep View/Swiss-PdbViewer (Peitsch 1996; Guex & Peitsch, 1997). Model of the ATPase domain of the $DnaK_{Mm}$ protein was done with the *E. coli* structure (1DKGD) used as a template. After modeling, the structures of the *M. mazei* proteins were minimized with the GROMOS96 force field implementation of Swiss-PdbViewer.

Fourier-transform infrared spectroscopy. Preparation of protein samples and Fourier-transform infrared spectroscopy was carried out as described previously (Żmijewski *et al.*, 2007)

Size exclusion chromatography. Size-exclusion chromatography was performed using an Agilent HPLC 1100 system equipped with a diode array detector and a Zorbax GF-250 column (Agilent Biotechnologies). In all experiments Zorbax GF-250 was equilibrated with 50 mM Tris, pH 7.5, 100 mM KCl buffer. DnaK proteins (100 μg/100 μl, or as stated in figure legends) were incubated in the presence (3 mM ATP or 3 mM ADP+Pi) or in the absence of nucleotide, or in the presence of 200 nM peptide NR (NRLLLTG) in 50 mM Tris, pH 7.5, 50 mM KCl, and 10 mM $MgCl_2$, for at least 30 min; they were then injected onto an HPLC column (a 100 μl loop was used), and resolved with a 1-ml per minute flow rate. In the case of DnaK incubated with ATP, the nucleotide was included in the elution buffer (as described by Wawrzynów and Żylicz, 1995) or was omitted, as explained in the text. For each set of experiments, the column was calibrated (in the presence or absence of ATP) with the following Sigma molecular-mass standards: bovine thyroglobulin (669 kDa), apoferritin from horse spleen (443 kDa), yeast alcohol dehydrogenase (150 kDa), and ovalbumin (45 kDa). Spectra were collected at 230, 260, and 280

nm. For the final presentation of data the 230-nm spectra were chosen, because $DnaK_{Mm}$ contains no tryptophan, and therefore shows low absorbance at 280 nm. Furthermore, the absorbance is poorly defined in the presence of ATP, which shows a maximum absorbance at 296 nm.

Determination of fluorescence spectra. A Perkin-Elmer LS55 spectrofluorimeter, equipped with a thermoregulated cuvette holder with stirrer and a Julabo thermostat, was used to record fluorescence emission spectra. All experiments were performed in 0.5×0.5 cm quartz cuvettes at 25°C, in a buffer containing 25 mM Hepes pH 7.0, 100 mM KCl, and 10 mM $MgCl_2$. Kinetics of complex formation of acrylodan-labeled peptide a-p4 with DnaK was measured with the excitation wavelength set at 370 nm (bandpass 4.6 nm, with excitation slits set at 4.6 nm), and the spectra were recorded at 510 nm (bandpass 18.6 nm, with emission slits set at 18.6 nm) for 900 s at 25°C. The reaction was started by addition of DnaK at final concentrations ranging from 0.1 to 5 μM. The concentration of the acrylodan-labeled peptide was held constant in all experiments (200 nM), and the final volume of the reaction mixture was 400 μl.

Determination of k_{obs}, kinetic constants (k_{+1}, k_{-1} and K_d) and evaluation of kinetic measurements for the DnaK–a-p4 peptide binding. To determine the rate constants k_{+1} and k_{-1} for complex formation between $DnaK_{Ec}$ or $DnaK_{Mm}$ and acrylodan-labelled peptide a-p4, the apparent rate constants k_{obs} were calculated for 200 nM peptide a-p4 and increasing concentrations (0.1 to 5 μM) of DnaK. Collected data were fitted to a single exponential equation (1):

$$F(t)=\Delta F[1-\exp(-k_{on}t)]+F_0, \quad (1)$$

where k_{on} represents first-order rate constant, ΔF, amplitude and F_0, initial fluorescence.

For all tested concentrations of DnaK the error of fitting for k_{obs} was lower than 2% and fitting to a double-exponential equation resulted in an increase of fitting error. The k_{obs} values were plotted against concentration of DnaK protein and data were fitted to the linear function. The association (k_{+1}) and dissociation (k_{-1}) rate constants were calculated according to equation (2):

$$K_{obs} = k_{+1}[\text{DnaK}]+k_{-1} \quad (2).$$

The dissociation equilibrium constants (K_d) of $DnaK_{Mm}$–a-p4 and $DnaK_{Ec}$–a-p4 complexes were calculated according to equation (3):

$$K_d=k_{-1}/k_{+1} \quad (3).$$

All calculations were performed with Origin 7.5 software (similar results for $DnaK_{Ec}$ were obtained with the Dynafit program).

Assay of σ^{32} levels. *E. coli* strains were transformed with appropriate plasmids according to (Sambrook *et al.*, 1989). The transformed bacteria were grown in LB medium with aeration at 30°C to an OD_{595} of 0.6, and then were heat-shocked at 45°C for 1 h. The heat shock was followed by a 1-h recovery period at 30°C. Equivalent amounts of each culture were harvested before and after heat shock, and after the recovery period, and were analyzed by 12.5% SDS/PAGE followed by Western blotting with anti-σ^{32} antibodies.

Enzyme-linked immunosorbent assay (ELISA). The ELISA assays were performed as described (Krzewski *et al.*, 2003), with some modification. Briefly, microtiter multiwell assay plates (Costar 3590) were coated with 0.5 μg of σ^{32} or BSA per well in 50 μl of PBS buffer, and were allowed to incubate overnight. Wells were washed four times with PBS buffer (0.17 M NaCl, 5 mM KCl, 10 mM Na_2HPO_4; 7 mM KH_2PO_4) containing 0.1% BSA (PBS/BSA), and were then washed with binding buffer (25 mM Hepes/KOH, pH 7.5, 150 mM KCl, 10 mM $MgCl_2$, 0.1 mM EDTA, 2 mM DTT, 5% (v/v) glycerol, 0.05% Triton X-100, and 0.2% BSA). They were then incubated with serial dilutions of $DnaK_{Ec}$ or $DnaK_{Mm}$ protein (0.2–0.003125 μg/ml) in the binding buffer for 1 h. The glutaraldehyde cross-linking step was omitted. The wells were washed with binding buffer and four times with PBS/BSA. Anti-$DnaK_{Ec}$ (Wawrzynow & Zylicz, 1995) or anti-$DnaK_{Mm}$ (Clarens *et al.*, 1995) rabbit polyclonal antibodies were added (at 1:5000 dilution) in PBS/BSA for 2 h. Wells were washed four times with PBS/BSA, and then secondary antibodies (goat anti-rabbit IgG coupled with horseradish peroxidase) were added. Bound conjugates were detected colorimetrically, after 60 min incubation, by use of the horseradish peroxidase substrate tetramethylbenzidine (TMB). Each assay was repeated at least three times.

Surface plasmon resonance spectroscopy. Studies on interaction of DnaK proteins with σ^{32} were carried out by use of the BIAcore 2000 biosensor (Pharmacia Biosensor AB, Uppsala, Sweden) and determination of SPR changes. Research-grade CM5 chips were coated with σ^{32} to about 2000 resonance units (RU) using the EDC/NHS coupling kit (*N*-ethyl-*N*'-(dimethylaminopropyl)carbodiimide, *N*-hydroxysuccinimide; Pharmacia Biosense AB). The cell temperature was 25°C, and the running buffer was 50 mM Hepes (pH 7.5), 100 mM KCl, 10 mM $MgCl_2$, 0.005% (v/v) Tween 20. The $DnaK_{Ec}$ or $DnaK_{Mm}$ protein was passed over the σ^{32}-coated chip and an empty control chip with a flow rate of 10 μM/min at 1 μM concentrations. As a control, BSA was used with the same concentration and conditions. ATP (12.5 μM) was added at least 5 min before injection. The signal obtained from the non-coated chip was subtracted from the signal obtained from the chip with coupled σ^{32}. The σ^{32}-coupled chip was regenerated by the addition of 20 μl of 1 M urea at a flow

rate of 10 μl/min. Spectra were evaluated with the software supplied with the BIAcore instrument.

RESULTS

Binding of substrates by $DnaK_{Mm}$ and $DnaK_{Ec}$

In our previous work we demonstrated that $DnaK_{Mm}$ has a chaperoning capacity comparable to that of $DnaK_{Ec}$; however, the substrate (polypeptide)-binding properties of the archaeal protein were not investigated (Żmijewski *et al.*, 2004). In this work, substrate binding was assessed to determine whether or not $DnaK_{Mm}$ and $DnaK_{Ec}$ differ in specificity. For this purpose, we compared the abilities of the two proteins to bind the acrylodan-labeled peptide a-p4 (a-CALLQSRLLS), a known $DnaK_{Ec}$ substrate successfully used for kinetic measurements (Gisler *et al.*, 1998). We measured by spectrofluorometry the kinetics of the binding of the a-p4 peptide by the two DnaKs, and then used the data to calculate the kinetic constants, as described under Materials and Methods. The results are shown in Fig. 1 (k_{obs} values plotted against DnaK concentrations); Table 2 shows the calculated kinetic constants. The k_{+1} values were significantly different for the two proteins, indicating that the chaperone–a-p4 peptide complex formation was considerably slower (by approx. 8-fold, in the experiment shown) for $DnaK_{Mm}$ than for $DnaK_{Ec}$. The dissociation equilibrium constants (K_d) differed between the two chaperones to a smaller extent, showing nonetheless that binding of the peptide to $DnaK_{Mm}$ was at least 2-fold weaker (e.g., 0.91 μM for $DnaK_{Ec}$ *vs.* 2.57 μM for $DnaK_{Mm}$).

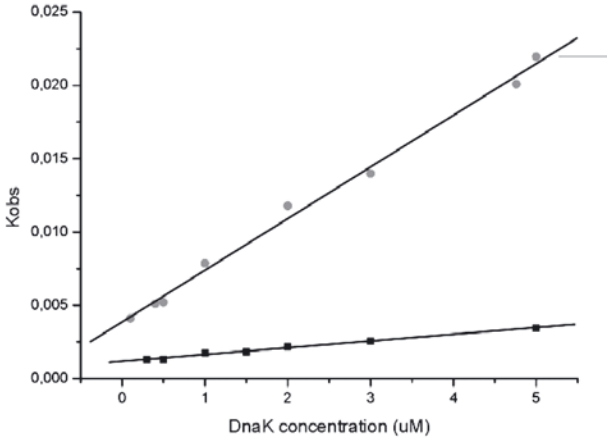

Figure 1. Kinetics of peptide binding by DnaK proteins. To follow the binding of the test polypeptide to the chaperone, we added $DnaK_{Mm}$ or $DnaK_{Ec}$ to the assay buffer containing acrylodan-labeled a-p4 (a-CALLQSRLLS) and measured the increase of acrylodan fluorescence with time, as described under Materials and Methods. Final concentrations were: a-p4, 0.2 μM; DnaK, 0.01–5 μM. The binding curves obtained were fitted to a single exponential function, and the k_{obs} values were derived for $DnaK_{Ec}$ (circles) and $DnaK_{Mm}$ (squares). The k_{obs} values were plotted as a function of DnaK concentration; the plots were obtained from least-squares fitting of the data to an equation for a straight line.

The differences in the substrate-binding properties between the archaeal and bacterial chaperones must be due to fine structural differences, most importantly those occurring in the substrate-binding domain (SBD). Our modeling of $DnaK_{Mm}$ showed a high degree of similarity between the SBDs of the *M. mazei* and *E. coli* proteins (Żmijewski *et al.*, 2007). However, close examination of the substrate-binding cavities of the two DnaKs revealed that the highly conserved methionine 404 in $DnaK_{Ec}$, forming an arch over the cavity, is replaced in $DnaK_{Mm}$ by leucine 378. Also, in the latch region, $DnaK_{Ec}$ histidine 544 is replaced in $DnaK_{Mm}$ by asparagine 518, and $DnaK_{Ec}$ aspartic acid 540 is replaced in $DnaK_{Mm}$ by glutamic acid 514 (Fig. 2A, B).

$DnaK_{Mm}$ is unable to down-regulate the *E. coli* heat-shock transcription factor σ^{32} *in vivo*

In *E. coli*, $DnaK_{Ec}$ participates in its own regulation, by interacting with the transcription factor σ^{32} and steering it toward degradation, which results in down-regulation of the *dnaK* gene when the cellular need for this chaperone diminishes. To find out whether $DnaK_{Mm}$ is able to interact with σ^{32} in the cell, we investigated whether $DnaK_{Mm}$ can down-regulate σ^{32} in *E. coli*, as $DnaK_{Ec}$ does. We used *E. coli* strains lacking DnaK (*E. coli* Δ*dnaK)* and strains that produce a mutant DnaK protein that lacks the self-regulatory ability (*E. coli dnaK756)*; both of these strains are unable to shut off the heat-shock response, in contrast to the wild-type. These strains were transformed with plasmids bearing the gene coding for $DnaK_{Mm}$ or the genes encoding $DnaK_{Mm}$ and $DnaJ_{Mm}$. We carried out the experiment with both the $dnaK_{Mm}$ and $dnaJ_{Mm}$ genes to rule out the possibility that a lack of $DnaK_{Mm}$ function was caused by a poor cooperation of $DnaK_{Mm}$ with $DnaJ_{Ec}$. The level of σ^{32} protein in cell lysates from the transformants was assessed by Western blotting (Fig. 3A). We also confirmed the presence of $DnaK_{Mm}$ in the transformants by Western blotting (not shown). Neither the presence of the $dnaK_{Mm}$ gene alone nor the presence of both genes from *M. mazei*, $dnaK_{Mm}$ and $dnaJ_{Mm}$, in the transformed mutant *E. coli* cells, caused a decrease in the levels of σ^{32} under heat shock conditions (when σ^{32} is elevated). In mutant *E. coli* cells transformed with a plasmid carrying $dnaK_{Ec}$ alone, or transformed with plasmids carrying both *E. coli* genes, $dnaK_{Ec}$ and $dnaJ_{Ec}$, the σ^{32} protein was barely detectable or undetectable, as expected. Likewise, in

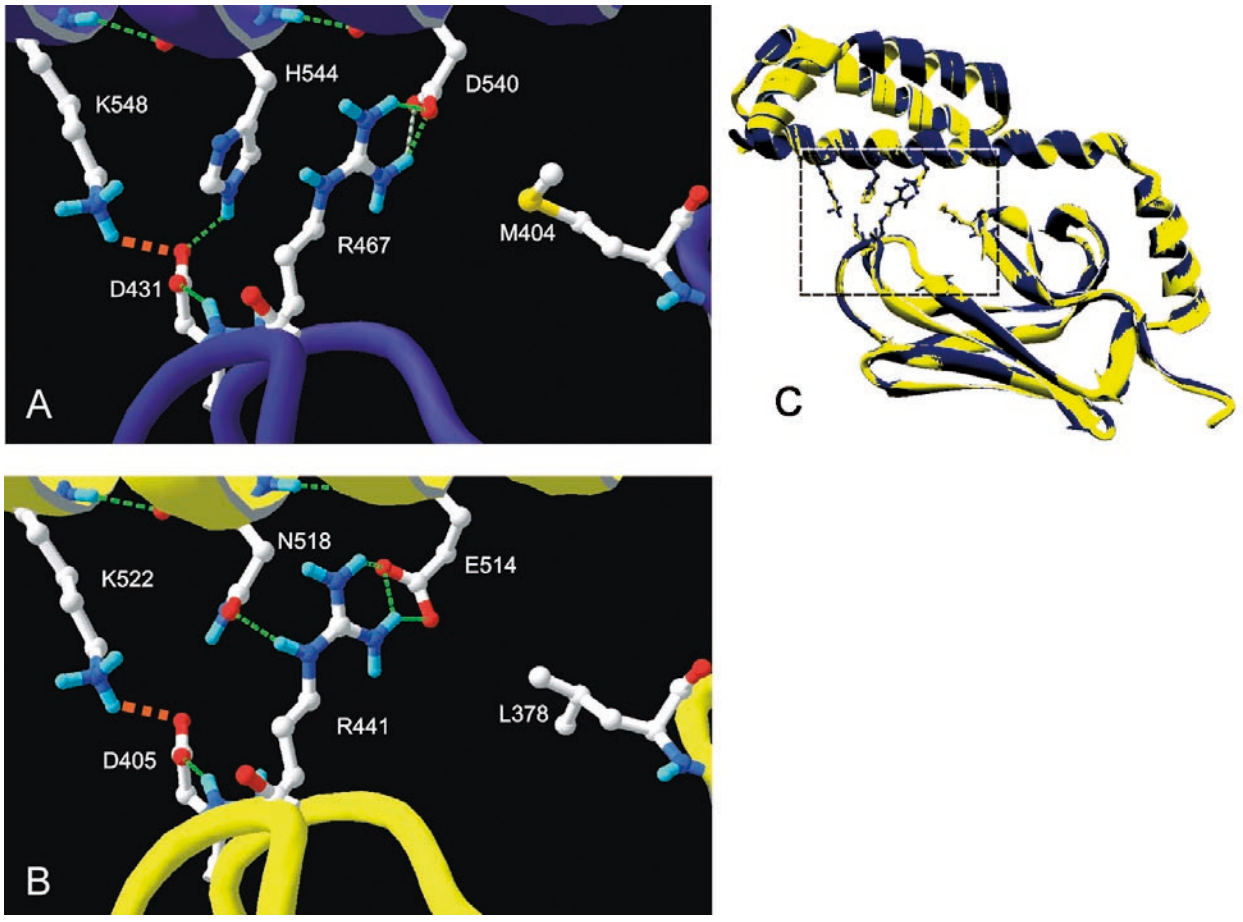

Figure 2. Putative differences between the substrate-binding domains of the archaeal and bacterial DnaKs. Shown are the latch regions (see the boxed structure in **C**) in the $DnaK_{Ec}$ SBD structure (**A**) and in the $DnaK_{Mm}$ SBD model (**B**), with some amino acids displayed in ball-and-stick format. Methionine (M404) in $DnaK_{Ec}$, forming an arch over peptide-binding cavity, is replaced by L378 in $DnaK_{Mm}$. Other appreciable differences at critical positions are H544 and D540 in $DnaK_{Ec}$, which are replaced in $DnaK_{Mm}$ by N518 and E514, respectively. Also shown are the salt bridges (orange) between K548 and D431 in $DnaK_{Ec}$ and K522 and D405 in $DnaK_{Mm}$, and hydrogen bonds (green) between amino acids of the α-helix and the outer loops $L_{4,5}$ and $L_{5,6}$; these salt bridges and hydrogen bonds are believed to stabilize the latch in $DnaK_{Ec}$ (Moro *et al*., 2004). (**C**) The substrate binding domain (SBD) of DnaK, with the latch region marked by a box.

the control, wild-type bacterium with its own *dnaK* gene (*E. coli* B178), the σ^{32} protein was undetectable. These results taken together indicate that $DnaK_{Mm}$ did not negatively regulate the σ^{32} transcription factor in *E. coli*, presumably because the chaperone was unable to bind the transcription factor, contrary to what happens with $DnaK_{Ec}$.

$DnaK_{Mm}$ poorly interacts with *E. coli* heat shock transcription factor σ^{32} *in vitro*

In order to check whether $DnaK_{Mm}$ is unable to physically interact with σ^{32} as efficiently as $DnaK_{Ec}$ does, we compared the binding capacities of $DnaK_{Mm}$ and $DnaK_{Ec}$ to *E. coli* σ^{32}, by applying an enzyme-linked immunosorbent assay (ELISA) and surface plasmon resonance (SPR) spectroscopy. In ELISA, we determined the amount of DnaK protein bound to σ^{32} immobilized on the plate wells, using anti-DnaK antibodies. The amount of $DnaK_{Mm}$ bound to σ^{32} was significantly lower than that of $DnaK_{Ec}$ (Fig. 3B). Reverse experiments were also performed. In these, the DnaK proteins were immobilized onto the ELISA-plate wells first, and then they were incubated with serial dilutions of σ^{32}; this was followed by detection of bound transcription factor with anti-σ^{32} antibodies. The results, not shown, were essentially the same as those obtained with immobilized σ^{32}, displayed in Fig. 3B.

The kinetics of interaction of either DnaK with immobilized σ^{32} protein was measured by SPR spectroscopy. $DnaK_{Mm}$ interacted with σ^{32} poorly as compared with $DnaK_{Ec}$ (Fig. 3C). In conclusion, the ELISA and SPR spectroscopy results showed that the $DnaK_{Mm}$ interaction with *E. coli* σ^{32} *in vitro* was considerably weaker than the interaction of $DnaK_{Ec}$ with the same factor. This finding is in agreement with the observed inabil-

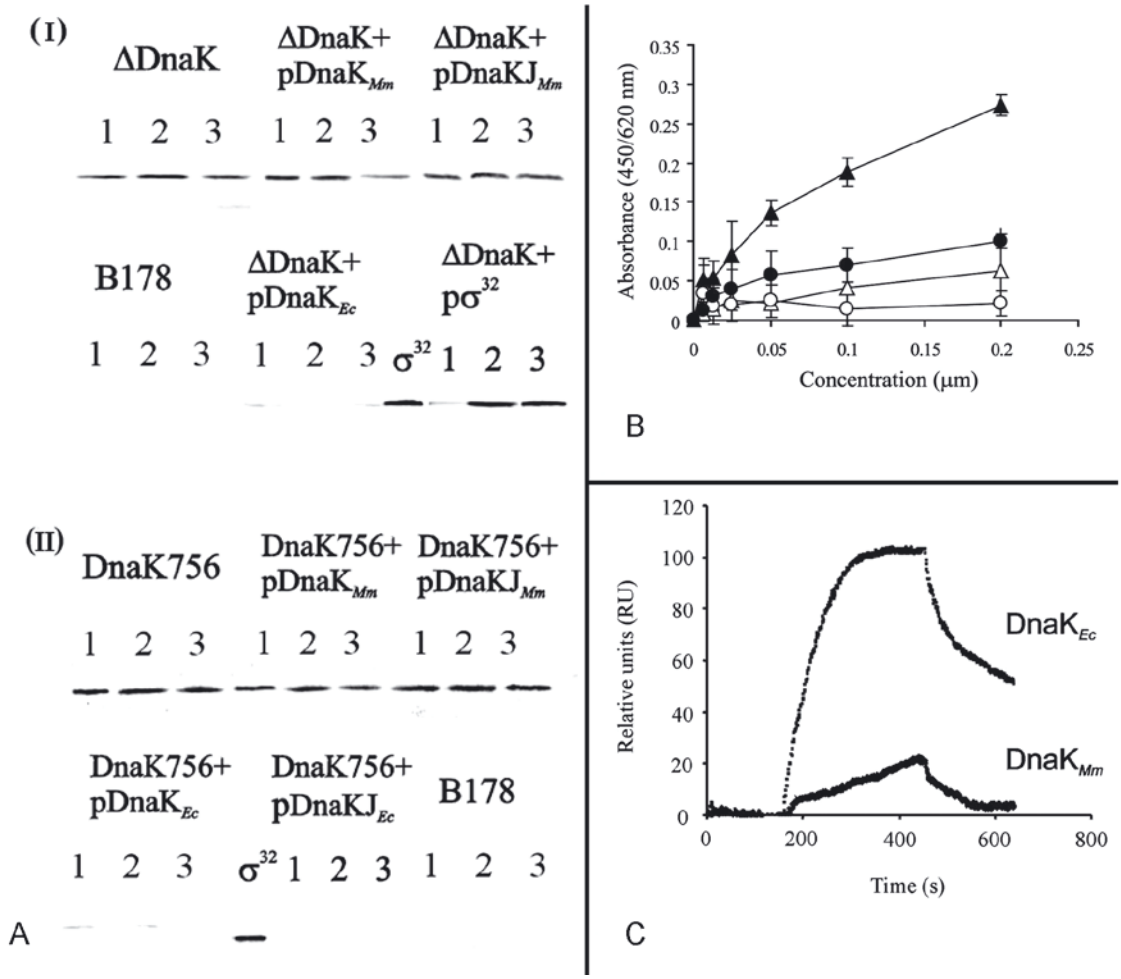

Figure 3. Archaeal DnaK does not down-regulate bacterial σ^{32} transcription factor.
(A) Western blotting results. *E. coli* Δ*dnaK* (I), or *E. coli dnaK*756 (II) bacteria were transformed with the plasmid pAM1-*dnaK*$_{Mm}$ or with the plasmid pAM3-*dnaKJ*$_{Mm}$. As positive controls, the *E. coli* B178 (*dnaK*$^{+}$) strain and the mutant strains transformed with the plasmids pMOB45-*dnaK*$_{Ec}$ or pJZ-589-*dnaK*$_{Ec}$*dnaJ*$_{Ec}$, were used. The *E. coli* Δ*dnaK* strain transformed with pAK1-*rpoH* plasmid (Δ*DnaK* + σ^{32}) and purified σ^{32} protein (σ^{32}) were included to show the position of σ^{32} in the gels. The various combinations tested are indicated above the corresponding lanes. *E. coli* was grown at 30°C, then heat-shocked at 45°C and the heat shock was followed by a recovery period at 30°C. Equivalent amounts of each culture were harvested before (1) and (2) after heat shock, and after the recovery period (3), and were analyzed by 12.5% SDS/PAGE followed by immunodetection with anti-σ^{32} antibodies. (B) Enzyme-linked immunosorbent assay (ELISA). Shown are binding curves produced by a series of concentrations of DnaK$_{Ec}$ and DnaK$_{Mm}$ and a constant amount of immobilized σ^{32} (closed triangles and circles, respectively), and bovine serum albumin (open triangles and circles). Mean values of at least three independent assays are presented; error bars represent standard deviations. (C) Surface plasmon resonance (SPR). In the example shown, 1 μM of DnaK$_{Mm}$ or DnaK$_{Ec}$ was passed over immobilized σ^{32} in the presence of 12.5 μM ATP, as described under Materials and Methods. The data were normalized, and the DnaK$_{Ec}$-σ^{32} maximum reading was set as 100 relative units. The same results were obtained in two other independent runs: the three sets of data were collinear, with variations not exceeding 5%.

ity of DnaK$_{Mm}$ to negatively regulate the σ^{32} levels *in vivo*.

Purified DnaK$_{Mm}$ exists predominantly in oligomeric forms

It is known that oligomerization status modulates chaperoning ability, e.g. in small heat-shock proteins (Narberhaus, 2002; Franzmann *et al.*, 2005), in eukaryotic Hsp70 (Blond-Elguindi *et al.*, 1993), and in some bacterial DnaKs (Motohashi *et al.*, 1994; Schonfeld *et al.*, 1995). Searching for differences in quaternary structure which might contribute to the differences in substrate binding by DnaK$_{Mm}$ and DnaK$_{Ec}$ we performed experiments to elucidate whether the archaeal chaperone oligomerizes under conditions resembling those *in vivo*.

Size-exclusion chromatography showed that DnaK$_{Mm}$ formed oligomers over a broad range of concentrations (0.1–5 mg/ml). The high-molecular mass oligomeric forms of DnaK$_{Mm}$ were predominant under all tested conditions, even at the lowest

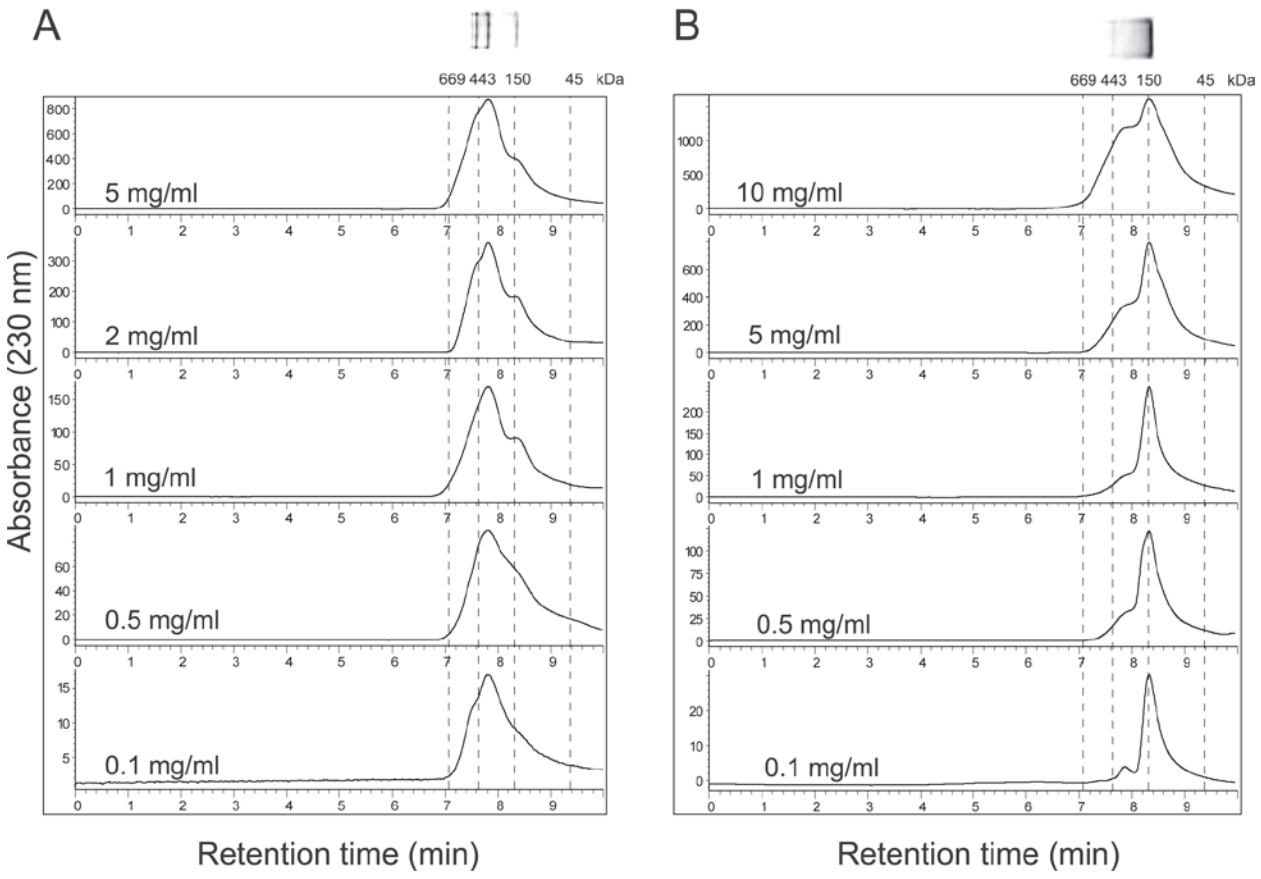

Figure 4. DnaK$_{Mm}$ and DnaK$_{Ec}$ differ in oligomerization state.
DnaK$_{Mm}$ **(A)** and DnaK$_{Ec}$ **(B)** were examined, in the absence of ATP, at various concentrations (10–1000 μg in 100-μl volumes) by size exclusion chromatography. Shown are UV spectra of the effluent at 230 nm. Above the panels are the respective electrophoregrams obtained with 5 μg of DnaK, using 10% PAGE under non-denaturing conditions. The mobilities of the molecular-mass standards, as resolved by HPLC under the same conditions, are indicated by vertical lines, with the corresponding molecular masses in kDa shown above each line.

protein concentration, as shown by high-pressure liquid chromatography (HPLC) (Fig. 4A). DnaK$_{Mm}$ showed the coexistence of three major forms, eluting as proteins with molecular masses of 440, 300 and 135 kDa; the ratio of these forms changed very little with concentration (these molecular masses represent mean values calculated from the results of five independent experiments; molecular-mass standards were run in each experiment). DnaK$_{Ec}$ subjected to HPLC under similar conditions showed substantial aggregation only at high (non-physiological) concentrations (5–10 mg/ml), and the lowest-molecular-mass form (eluting as a 140–150 kDa protein) was predominant within the range of 0.1–5 mg/ml (Fig. 4B). SDS/PAGE of the fractions containing a mixture of all the various DnaK forms did not resolve these forms, but showed the bands for DnaK$_{Mm}$ and DnaK$_{Ec}$ monomers (not shown).

The smallest DnaK$_{Ec}$ and DnaK$_{Mm}$ forms eluted (by HPLC) as species larger than 100 kDa. We assume that the 130–140 kDa form of DnaK$_{Mm}$ is the monomer, since it eluted like the smallest DnaK$_{Ec}$ form, and did not change its position upon ATP addition, when high-molecular-mass forms dissociated (Fig. 5A). Other investigators have also noticed that DnaK$_{Ec}$ does not behave like a 70 kDa globular protein should (Zylicz & Georgopoulos, 1984; A. Żylicz, personal communication). The presence of at least three forms with different molecular masses and the predominance of the high molecular-mass forms in the DnaK$_{Mm}$ preparations were confirmed by native gel electrophoresis (Fig. 5C, lanes 3, 8). In contrast, under the same experimental conditions, the low molecular-mass forms predominated in the DnaK$_{Ec}$ preparations (Fig. 5C, lanes 1, 7).

In order to investigate whether the DnaK$_{Mm}$ oligomerization has a functional significance with regard to the ATP cycle and substrate binding, we preincubated DnaK$_{Mm}$ with ATP, ADP+Pi, or the peptide NRLLLTG (NR), and then carried out size-exclusion chromatography. In these experiments we used the NR peptide as a model substrate, since it has previously been shown to efficiently bind DnaK (Gragerov *et al*., 1994; Buczynski *et al*., 2001).

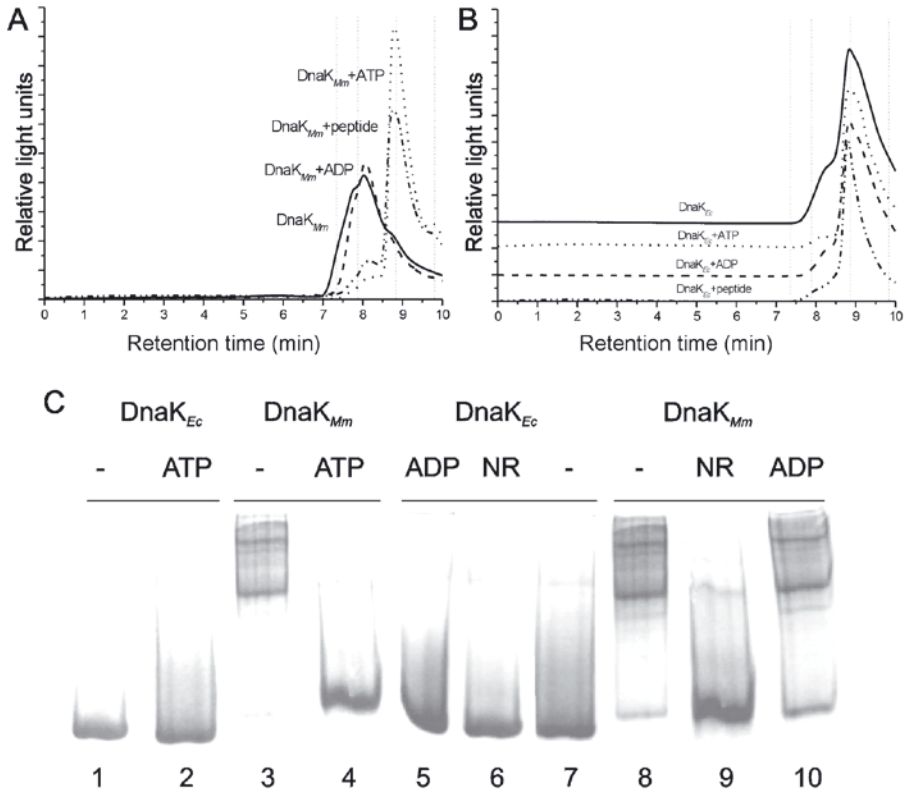

Figure 5. Effects of ATP, ADP, and substrate on DnaK oligomerization state.
(A, B) size-exclusion chromatography**.** DnaK$_{Mm}$ **(A)** or DnaK$_{Ec}$ **(B)** was incubated in the presence or absence of ATP, or ADP+Pi , or in the presence or absence of NR peptide (NRLLLTG) , as indicated. The incubated mixtures were resolved by size-exclusion chromatography and the UV spectra at 230 nm of the effluents are shown. For clarity, the spectra for DnaK$_{Ec}$ are displayed at different heights; otherwise, they would be indistinguishable, due to their great similarity. In contrast, the spectra for the various mixtures including DnaK$_{Mm}$ differ considerably from one another and are displayed at the same level. **(C)** PAGE. DnaK$_{Mm}$ or DnaK$_{Ec}$ was incubated for 30 min in the presence or absence (the latter indicated by a minus sign above the lane) of ATP, ADP+Pi or peptide NR (NRLLLTG), as shown. The incubated mixtures were analyzed by 10% PAGE under non-denaturing conditions. Lanes 1–4 and 5–10 are from two separate gels in which the controls DnaK$_{Mm}$ and DnaK$_{Ec}$ without additives were repeated (lanes 1, 3, 7, and 8).

In the presence of ATP or NR, the high-molecular-mass oligomers dissociated, and the majority of DnaK$_{Mm}$ eluted as about 140 kDa protein (Fig. 5A). In a similar experiment with DnaK$_{Ec}$, the major peak eluted as an about 130 kDa protein. Also, the small shoulder on the ascending portion of the curve, representing oligomers, decreased in magnitude in the presence of ATP (Fig. 5B), as expected from previous knowledge on dissociation of DnaK$_{Ec}$ (Palleros *et al.*, 1993). The elution profile of DnaK$_{Mm}$ preincubated with ATP was identical in the absence (Fig. 5A) and in the presence (not shown) of ATP in the elution buffer, which reflects the stability of the DnaK$_{Mm}$–ATP complex. Dissociation of DnaK$_{Mm}$ in the presence of ATP or NR was confirmed by native electrophoresis (Fig. 5C). The observed dissociation in the presence of ATP and a substrate suggests that the monomeric form of DnaK$_{Mm}$ may be the active form, participating in peptide binding. ADP, in contrast to ATP and NR, did not cause dissociation of the DnaK$_{Mm}$ oligomers (Fig. 5A and 5C, lane 10), which resembled the situation described for DnaK$_{Ec}$ (Palleros *et al.*, 1993).

Protein oligomerization may theoretically lead to a restricted accessibility of certain region(s) of a molecule to a solvent, which could result in a decreased access of the substrate to the protein. Our previous analysis of DnaK$_{Mm}$ by Fourier-transform infrared spectroscopy showed that the $^1H/^2H$ exchange of the amide hydrogens of the polypeptide chain was less complete than in the case of DnaK$_{Ec}$ (Żmijewski *et al.*, 2007). The extent of the $^1H/^2H$ exchange can be measured by monitoring the intensity of the residual amide II band (encompassing the 1600–1500 cm^{-1} interval) absorption, i.e., the absorption of the amide II band after the $^1H/^2H$ exchange. In ^1H_2O medium, the amide II band intensity was about 2/3 of the intensity of the amide I band (not shown). In ^2H_2O medium, the intensity of the amide II band decreases as a consequence of the ex-

Table 2. Rates of formation, and dissociation equilibrium constants, of DnaK$_{Mm}$ and DnaK$_{Ec}$ complexes with a-p4 (a-CALLQSRLLS) peptide

Protein	k_{obs} (s^{-1})[a]	k_{+1} ($M^{-1}s^{-1}$)[b]	k_{-1} (s^{-1})[b]	K_d (μM)[c]
DnaK$_{Mm}$	0.00176 (±0.0000016)	494 (±56)	0.00118 (±0.000137)	2.57 (±0.39)
DnaK$_{Ec}$	0.00786 (±0.00001)	3871 (±304)	0.00353 (±0.0001)	0.91 (±0.077)

[a]For 200 nM peptide a-p4 and 1 μM DnaK protein. [b]The rate constants k_{+1} and k_{-1} were determined by titration of acrylodan-labeled peptide a-p4 with increasing concentrations of DnaK (see Fig. 1). [c]Dissociation equilibrium constant K_d was calculated from ratio k_{+1}/k_{-1}. For details on the determination of k_{obs} and the kinetic constants, see Materials and Methods.

change of amide hydrogens with deuterium (Osborne & Nabedryk-Viala, 1982; D'Auria *et al*., 2004). The larger the decrease in intensity of the amide II band, the larger the $^1H/^2H$ exchange and, in turn, the greater the accessibility of the solvent (^2H_2O) to the protein. Fig. 6A, B shows the temperature-dependent changes of the DnaK$_{Mm}$ and DnaK$_{Ec}$ infrared absorbance spectra in the 1600–1500 cm^{-1} interval. At 20°C the absorbance of DnaK$_{Mm}$ close to 1550 cm^{-1} is higher than in the DnaK$_{Ec}$ spectrum, indicating a lower accessibility of ^2H_2O to DnaK$_{Mm}$. A temperature increase causes a decrease of absorption close to 1550 cm^{-1} (residual amide II band) due to a further $^1H/^2H$ exchange, a consequence of temperature-dependent molecular dynamics and/or protein denaturation. A more detailed comparison was possible when the $^1H/^2H$ exchange as a function of temperature was calculated, Fig. 6C, as done previously (D'Auria *et al*., 2004). Full $^1H/^2H$ exchange was reached by DnaK$_{Mm}$ at higher temperatures compared to DnaK$_{Ec}$ and the temperature at which a full exchange occurred can be estimated to be 55–60°C for DnaK$_{Ec}$ and about 65°C for DnaK$_{Mm}$ (Fig. 6C), the temperatures corresponding approximately to the melting points (Tms) previously calculated for DnaK$_{Ec}$ and DnaK$_{Mm}$, respectively (Żmijewski *et al*., 2007). On the other hand, the maximum rate of exchange (midpoint of the $^1H/^2H$ exchange curves) was

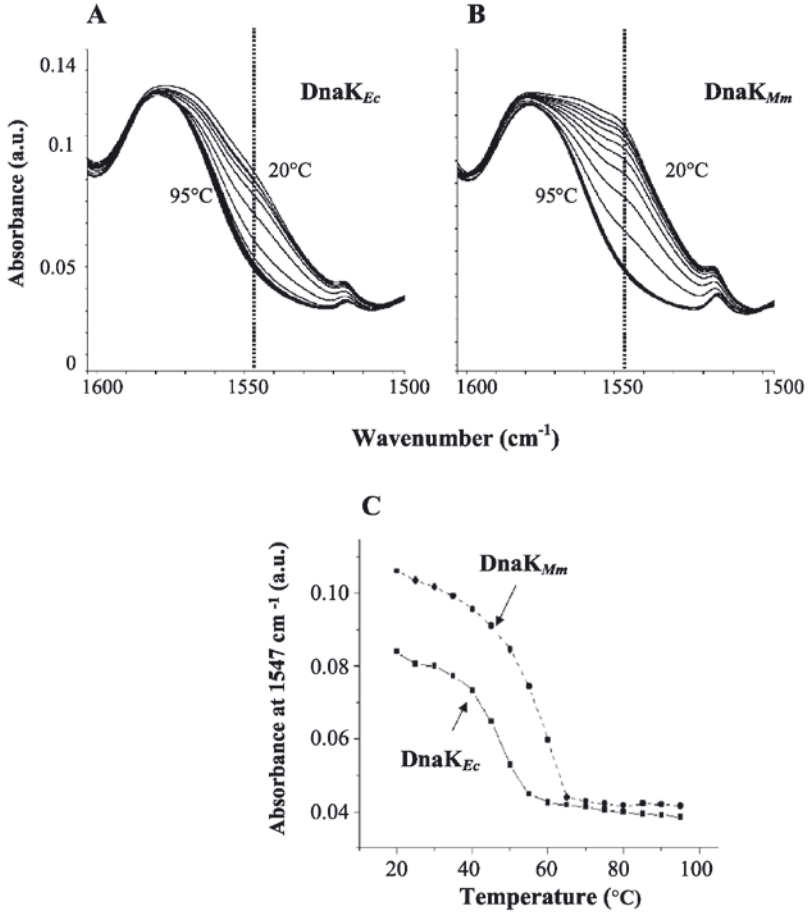

Figure 6. Fourier-transform infrared spectroscopy results. (**A, B**) Temperature-dependent changes of DnaK$_{Mm}$ (B) and DnaK$_{Ec}$ (A) absorbance spectra in the range encompassing amide II band. The graphs display the absorbance spectra of DnaK$_{Mm}$ and DnaK$_{Ec}$ at 20, 30, 40, 50, 60, 70, 80, and 95°C. The vertical dotted lines indicate position of the peak at 1547 cm^{-1}. These spectra were used to calculate the proteins' $^1H/^2H$ exchanges, shown in (C) (**C**) $^1H/^2H$ exchange curves of DnaK$_{Mm}$ (circles) and DnaK$_{Ec}$ (squares), respectively. The maximum rate of $^1H/^2H$ exchange (midpoint of the $^1H/^2H$ exchange curves) was calculated from the curves as described (Meersman *et al*., 2002). The maximum rate of $^1H/^2H$ exchange is at 54.8 for DnaK$_{Mm}$, and at 46.3 °C for DnaK$_{Ec}$. All determinations and the calculation of arbitrary units (a.u.) were done as described in Materials and Methods.

calculated to occur at 46.3 for $DnaK_{Ec}$ and at 54.8°C for $DnaK_{Mm}$. The analysis of $^1H/^2H$ exchange thus indicates that $DnaK_{Mm}$ is less accessible to the solvent than is $DnaK_{Ec}$ and that the proteins undergo maximum rate of $^1H/^2H$ exchange at temperatures much lower than the corresponding Tms, temperatures at which the exchange is almost complete.

DISCUSSION

It has been shown previously that there is a high functional similarity between the DnaK of *M. mazei* and DnaK of *E. coli* (Żmijewski *et al.*, 2004), which is based on the overall structural similarity of these proteins (Żmijewski *et al.*, 2007). In spite of these similarities, there is a significant functional difference, indicated by the fact that the *dnaK* gene of *M. mazei* is unable to complement *dnaK* mutations in *E. coli* (Żmijewski *et al.*, 2004). To better understand the molecular basis of the observed species-specificity, we compared substrate binding by the *M. mazei* and *E. coli* DnaK proteins. We used two types of substrates: (1) a peptide, which represents DnaK general substrates — unfolded proteins, and (2) *E. coli* sigma 32 transcription factor, a protein which is bound by $DnaK_{Ec}$ in its native (folded) state.

$DnaK_{Mm}$ differed from $DnaK_{Ec}$ in its affinity for the substrate, peptide ap-4 (acrylodan-labeled CALLQSRLLS) (Fig. 1 and Table 2). SBD modeling of $DnaK_{Mm}$ showed a high similarity of this domain to SBD of $DnaK_{Ec}$ (Żmijewski *et al.*, 2007) but also predicted small differences in the latch region, which could influence the closing and opening rates of the $DnaK_{Mm}$. For example, the highly conserved methionine 404, forming an arch over the substrate-binding cavity in $DnaK_{Ec}$, is absent in $DnaK_{Mm}$; $DnaK_{Ec}$ histidine 544 is replaced in $DnaK_{Mm}$ by asparagine 518, and $DnaK_{Ec}$ aspartic acid 540 is replaced in $DnaK_{Mm}$ by glutamic acid 514 (Fig. 2A, B). According to (Rudiger *et al.*, 2000), even small changes in this region of $DnaK_{Ec}$, in particular replacement of methionine 404 by another amino acid, will modify substrate-specificity. Recently, it has been demonstrated that interactions forming the latch are critical in maintaining DnaK functional cycle, because their disruption renders the protein unable to refold protein substrates (Fernandez-Saiz *et al.*, 2006). Thus, it is likely that the putative structural differences between the $DnaK_{Mm}$ SBD and that of $DnaK_{Ec}$ revealed by the model, do operate in reality, and that they contribute to the observed lower affinity of $DnaK_{Mm}$ for the substrate (Fig. 1, and Table 2). It has been shown previously that Hsp70s from different organisms recognize peptide substrates with differing affinities (Fourie *et al.*, 1994), a fact which could be attributed to amino-acid substitutions within the DnaK substrate-binding cavity and in the lid region (Mayer *et al.*, 2000). It is possible that different affinity of $DnaK_{Mm}$ for unfolded protein substrates could be one of the reasons why it is unable to substitute for $DnaK_{Ec}$ in a cell.

$DnaK_{Mm}$ interacted poorly, if at all, with *E. coli* σ^{32}, a natural ligand for $DnaK_{Ec}$, and it did not negatively regulate the σ^{32} level in *E. coli* cells (Fig. 3). The observed lack of σ^{32} down-regulation is not likely to be the reason why $DnaK_{Mm}$ does not suppress the thermosensitivity of the *E. coli dnaK* mutants. High levels of σ^{32} promote transcription of heat shock genes which should help bacterium survive at high temperatures (Yura & Nakahigashi, 1999). However, there may be other native proteins, as yet unidentified, which are substrates for $DnaK_{Ec}$, and whose binding is essential for bacterial survival at elevated temperatures. The failure to recognize such proteins by $DnaK_{Mm}$ would result in its inability to suppress the thermosensitivity of the *E. coli* bacteria without a functional $DnaK_{Ec}$. Mogk and coworkers (1999) showed that DnaK from the Gram-positive bacterium *Bacillus subtilis*, a protein that is very close to $DnaK_{Mm}$ in phylogenetic trees and shows a high percentage of identical amino acids, did not have the ability to cause degradation of σ^{32}. They found that the degradation-promoting activity depends on the integrity of a carboxy-terminal $DnaK_{Ec}$ region (about 10 kDa, encompassing amino acids 543–637). While the primary sequence of this small region is the least-conserved portion of the DnaK proteins (about 35% identity), the putative three-dimensional structures of this region do not differ appreciably between $DnaK_{Mm}$ and $DnaK_{Ec}$ (Żmijewski *et al.*, 2007). It remains to be determined which amino acids in the carboxy-terminal region of $DnaK_{Ec}$ are directly involved in σ^{32} binding and unfolding, the processes that precede degradation of the transcription factor.

Searching for differences in the quaternary structure which might contribute to the differences in substrate binding, we performed size-exclusion chromatography and native gel electrophoresis, and found that $DnaK_{Mm}$ occurred in solution mainly as high-molecular-mass oligomeric forms (Fig. 4), and that these forms dissociated upon ATP or peptide binding (Fig. 5). Under the same conditions, $DnaK_{Ec}$ formed smaller oligomers, in smaller quantities. It is possible that dissociation of the $DnaK_{Mm}$ oligomers is necessary for full activation of the chaperone, as has been postulated for DnaK from the bacterium *Thermus thermophilus* (Watanabe & Yoshida, 2004). Moreover, it has been shown that the monomeric form of $DnaK_{Ec}$ is fully active

(Palleros *et al.*, 1993). Furthermore, the ATP-driven monomerization has been shown to occur for the eukaryotic DnaK homologs Hsp70 and Hsc70, and it has been suggested that the non-aggregated forms exert the chaperone activity (Angelidis *et al.*, 1999). It is possible that formation of highly oligomeric forms by $DnaK_{Mm}$ decreases the efficiency of substrate binding/releasing and thus may be one of the reasons why $DnaK_{Mm}$ functioning in *E. coli* cell is impaired. The FTIR analysis of the $^1H/^2H$ exchange of the amide hydrogens of the polypeptide chain indicated that $DnaK_{Mm}$ is less accessible to the solvent than is $DnaK_{Ec}$ (Fig. 6). This might be caused by $DnaK_{Mm}$ oligomerization and could theoretically lead to a decreased access of the substrate to the protein. It can also be speculated that oligomerization of $DnaK_{Mm}$ may be part of an additional regulatory mechanism of DnaK function in *M. mazei*, and lack of this regulation in *E. coli* may contribute to the inefficient functioning of $DnaK_{Mm}$ in *E. coli* cells.

It is worth pointing out that this is the first study showing substrate binding by a purified archaeal DnaK and the first attempt to solve the species-specificity of an archaeal Hsp70. Furthermore, this work shows a new aspect of the archaeal DnaK protein, namely its highly oligomeric structure.

Acknowledgements

We would like to express our gratitude to Everly Conway de Macario for excellent advice and for critical readings of the manuscript. We are grateful to J.P. Christen for the generous gift of the acrylodan-labeled peptide a-p4 and his valuable advice, Z. Wasylewski and A. Gorecki for help with interpretation of the kinetic measurements, A. Żylicz for helpful discussion, I. Konieczny for help with SPR analysis, and the Photography and Illustration Unit of the Wadsworth Center for help with figures.

This work was supported by a grant from the Polish Committee for Scientific Research (KBN 374/P04/99/16), by a grant from Università Politecnica delle Marche (ricerche di Ateneo). The initial part of this work by A.J.L.M. was started at the Wadsworth Center, New York State Department of Health (Albany, New York, USA) partially supported by a grant from the San Francisco Foundation.

REFERENCES

Angelidis CE, Lazaridis I, Pagoulatos GN (1999) Aggregation of hsp70 and hsc70 *in vivo* is distinct and temperature-dependent and their chaperone function is directly related to non-aggregated forms. *Eur J Biochem* **259**: 505–512.

Blond-Elguindi S, Fourie AM, Sambrook JF, Gething MJ (1993) Peptide-dependent stimulation of the ATPase activity of the molecular chaperone BiP is the result of conversion of oligomers to active monomers. *J Biol Chem* **268**: 12730–12735.

Bradford MM (1976) A rapid and sensitive method for the quantitation of microgram quantities of protein utilizing the principle of protein-dye binding. *Anal Biochem* **72**: 248–254.

Buczynski G, Slepenkov SV, Sehorn MG, Witt SN (2001) Characterization of a lidless form of the molecular chaperone DnaK: deletion of the lid increases peptide on- and off-rate constants. *J Biol Chem* **276**: 27231–27236

Bukau B, Deuerling E, Pfund C, Craig EA (2000) Getting newly synthesized proteins into shape. *Cell* **101**: 119–122.

Bukau B, Weissman J, Horwich A (2006) Molecular chaperones and protein quality control. *Cell* **125**: 443–451.

Clarens M, Macario AJ, Conway de Macario E (1995) The archaeal *dnaK-dnaJ* gene cluster: organization and expression in the methanogen *Methanosarcina mazei*. *J Mol Biol* **250**: 191–201.

D'Auria S, Alfieri F, Staiano M, Pelella F, Rossi M, Scire A, Tanfani F, Bertoli E, Grycznyski Z, Lakowicz JR (2004) Structural and thermal stability characterization of *Escherichia coli* D-galactose/D-glucose-binding protein. *Biotechnol Prog* **20**: 330–337.

Deuerling E, Bukau B (2004) Chaperone-assisted folding of newly synthesized proteins in the cytosol. *Crit Rev Biochem Mol Biol* **39**: 261–277.

Erbse A, Mayer MP, Bukau B (2004) Mechanism of substrate recognition by Hsp70 chaperones. *Biochem Soc Trans* **32**: 617–621.

Fernandez-Saiz V, Moro F, Arizmendi JM, Acebron SP, Muga A (2006) Ionic contacts at DnaK substrate binding domain involved in the allosteric regulation of lid dynamics. *J Biol Chem* **281**: 7479–7488.

Fourie AM, Sambrook JF, Gething MJ (1994) Common and divergent peptide binding specificities of hsp70 molecular chaperones. *J Biol Chem* **269**: 30470–30478.

Franzmann TM, Wuhr M, Richter K, Walter S, Buchner J (2005) The activation mechanism of Hsp26 does not require dissociation of the oligomer. *J Mol Biol* **350**: 1083–1093.

Gisler SM, Pierpaoli EV, Christen P (1998) Catapult mechanism renders the chaperone action of Hsp70 unidirectional. *J Mol Biol* **279**: 833–840.

Gragerov A, Zeng L, Zhao X, Burkholder W, Gottesman ME (1994) Specificity of DnaK-peptide binding. *J Mol Biol* **23**: 848–854.

Gribaldo S, Lumia V, Creti R, de Macario EC, Sanangelantoni A, Cammarano P (1999) Discontinuous occurrence of the *hsp70* (*dnaK*) gene among *Archaea* and sequence features of HSP70 suggest a novel outlook on phylogenies inferred from this protein. *J Bacteriol* **181**: 434–443.

Guex N, Peitsch MC (1997) SWISS-MODEL and the Swiss-PdbViewer: an environment for comparative protein modeling. *Electrophoresis* **18**: 2714–2723.

Harrison CJ, Hayer-Hartl M, Di Liberto M, Hartl F, Kuriyan J (1997) Crystal structure of the nucleotide exchange factor GrpE bound to the ATPase domain of the molecular chaperone DnaK. *Science* **276**: 431–435.

Kedzierska S, Staniszewska M, Wegrzyn A, Taylor A (1999) The role of DnaK/DnaJ and GroEL/GroES systems in the removal of endogenous proteins aggregat-

ed by heat-shock from *Escherichia coli* cells. *FEBS Lett* **446**: 331–337.

Kotlarz A, Szalewska-Palasz A, Wegrzyn G, Lipinska B (1998) Economical and efficient overproduction of the *Escherichia coli* 32 transcription factor. *Biotechnol Tech* **12**.

Krzewski K, Kunikowska D, Wysocki J, Kotlarz A, Thompkins P, Ashraf W, Lindsey N, Picksley S, Głośnicka R, Lipińska B (2003) Characterisation of the anti-DnaJ monoclonal antibodies and their use to compare immunological properties of DnaJ and its human homologue HDJ-1. *Cell Stress Chaperones* **8**: 8–17.

Kultz D (2005) Molecular and evolutionary basis of the cellular stress response. *Annu Rev Physiol* **67**: 225–257.

Laemmli UK (1970) Cleavage of structural proteins during assembly of the head of bacteriophage T4. *Nature* **227**: 680–685.

Lanzetta PA, Alvarez LJ, Reinach PS, Candia OA (1979) An improved assay for nanomole amounts of inorganic phosphate. *Anal Biochem* **100**: 95–97.

Liberek K, Galitski TP, Zylicz M, Georgopoulos C (1992) The DnaK chaperone modulates the heat shock response of *Escherichia coli* by binding to the sigma 32 transcription factor. *Proc Natl Acad Sci USA* **89**: 3516–3520.

Macario AJ, Dugan CB, Conway de Macario E (1991) A dnaK homolog in the archaebacterium *Methanosarcina mazei* S6. *Gene* **108**: 133–137.

Macario AJ, Conway De Macario E (2001) The molecular chaperone system and other anti-stress mechanisms in archaea. *Front Biosci* **6**: D262–283.

Macario AJ, Malz M, Conway de Macario E (2004) Evolution of assisted protein folding: the distribution of the main chaperoning systems within the phylogenetic domain archaea. *Front Biosci* **9**: 1318–1332.

Mayer MP, Schroder H, Rudiger S, Paal K, Laufen T, Bukau B (2000) Multistep mechanism of substrate binding determines chaperone activity of Hsp70. *Nat Struct Biol* **7**: 586–593.

Mehlert A, Young DB (1989) Biochemical and antigenic characterization of the *Mycobacterium tuberculosis* 71kD antigen, a member of the 70 kD heat-shock protein family. *Mol Microbiol* **3**: 125–30.

Meersman F, Smeller L, Heremans K (2002) Comparative Fourier transform infrared spectroscopy study of cold-, pressure-, and heat-induced unfolding and aggregation of myoglobin. *Biophys J* **82**: 2635–2644.

Minder C, Narberhaus F, Babst M, Hennecke H, Fischer HM (1997) The dnaKJ operon belongs to the sigma32-dependent class of heat shock genes in *Bradyrhizobium japonicum*. *Mol Gen Genet* **254**: 195–206.

Mogk A, Bukau B, Lutz R, Schumann W (1999) Construction and analysis of hybrid *Escherichia coli-Bacillus subtilis dnaK* genes. *J Bacteriol* **181**: 1971–1974.

Moro F, Fernandez-Saiz V, Muga A (2004) The lid subdomain of DnaK is required for the stabilization of the substrate-binding site. *J Biol Chem* **279**: 19600–19606.

Motohashi K, Taguchi H, Ishii N, Yoshida M (1994) Isolation of the stable hexameric DnaK. DnaJ complex from *Thermus thermophilus*. *J Biol Chem* **269**: 27074–27079.

Narberhaus F (2002) Alpha-crystallin-type heat shock proteins: socializing minichaperones in the context of a multichaperone network. *Microbiol Mol Biol Rev* **66**: 64–93; table of contents.

Osborne HB, Nabedryk-Viala E (1982) Infrared measurements of peptide hydrogen exchange in rhodopsin. *Metods Enzymol* **88**: 676–680.

Paek KH, Walker GC (1987) *Escherichia coli* dnaK null mutants are inviable at high temperature. *J Bacteriol* **169**: 283–290.

Palleros DR, Reid KL, Shi L, Fink AL (1993) DnaK ATPase activity revisited. *FEBS Lett* **336**: 124–128.

Peitsch MC (1996) ProMod and Swiss-Model: Internet-based tools for automated comparative protein modelling. *Biochem Soc Trans* **24**: 274–279.

Rudiger S, Mayer MP, Schneider-Mergener J, Bukau B (2000) Modulation of substrate specificity of the DnaK chaperone by alteration of a hydrophobic arch. *J Mol Biol* **304**: 245–251.

Sambrook J, Frisch EF, Maniatis T (1989) *Molecular cloning: a laboratory manual*. Cold Spring Harbor Laboratory Press, New York.

Schonfeld HJ, Schmidt D, Schroder H, Bukau B (1995) The DnaK chaperone system of *Escherichia coli*: quaternary structures and interactions of the DnaK and GrpE components. *J Biol Chem* **270**: 2183–2189.

Sell SM, Eisen C, Ang D, Zylicz M, Georgopoulos C (1990) Isolation and characterization of *dnaJ* null mutants of *Escherichia coli*. *J Bacteriol* **172**: 4827–4835.

Sussman MD, Setlow P (1987) Nucleotide sequence of a *Bacillus megaterium* gene homologous to the *dnaK* gene of *Eschrichia coli*. *Nucleic Acids Res* **15**: 3923.

Szewczyk B, Harper DR (1994) Use of blotted proteins as immunogens. In *Protein blotting — a practical approach*. (D B ed) pp 189–205. Oxford University Press, Cary, NC.

Tabor S, Richardson CC (1985) A bacteriophage T7 RNA polymerase/promoter system for controlled exclusive expression of specific genes. *Proc Natl Acad Sci USA* **82**: 1074–1078.

Tilly K, Hauser R, Campbell J, Ostheimer GJ (1993) Isolation of *dnaJ*, *dnaK*, and *grpE* homologues from *Borrelia burgdorferi* and complementation of *Escherichia coli* mutants. *Mol Microbiol* **7**: 359–69.

Truscott KN, Brandner K, Pfanner N (2003) Mechanisms of protein import into mitochondria. *Curr Biol* **13**: R326–337.

Watanabe YH, Yoshida M (2004) Trigonal DnaK-DnaJ complex *versus* free DnaK and DnaJ: heat stress converts the former to the latter, and only the latter can do disaggregation in cooperation with ClpB. *J Biol Chem* **279**: 15723–15727.

Wawrzynow A, Zylicz M (1995) Divergent effects of ATP on the binding of the DnaK and DnaJ chaperones to each other, or to their various native and denatured protein substrates. *J Biol Chem* **270**: 19300–19306.

Wu B, Ang D, Snavely M, Georgopoulos C (1994) Isolation and characterization of point mutations in the *Escherichia coli grpE* heat shock gene. *J Bacteriol* **176**: 6965–6973.

Young JC, Agashe VR, Siegers K, Hartl FU (2004) Pathways of chaperone-mediated protein folding in the cytosol. *Nat Rev Mol Cell Biol* **5**: 781–791.

Yura T, Nakahigashi K (1999) Regulation of the heat-shock response. *Curr Opin Microbiol* **2**: 153–158.

Zhu X, Zhao X, Burkholder WF, Gragerov A, Ogata CM, Gottesman ME, Hendrickson WA (1996) Structural analysis of substrate binding by the molecular chaperone DnaK. *Science* **272**: 1606–1614.

Żmijewski MA, Macario AJ, Lipinska B (2004) Functional similarities and differences of an archaeal Hsp70(DnaK) stress protein compared with its homologue from the bacterium *Escherichia coli*. *J Mol Biol* **336**: 539–549.

Żmijewski MA, Skórko-Glonek, J, Tanfani, F, Banecki B, Kotlarz A, Macario AJL, Lipińska B (2007) Structural basis of the interspecies interaction between the chaperone DnaK(Hsp70) and the co-chaperone GrpE of archaea and bacteria. *Acta Biochim Polon* epub ahead of print (www.actabp.pl).

Zylicz M, Georgopoulos C (1984) Purification and properties of the *Escherichia coli* dnaK replication protein. *J Biol Chem* **259**: 8820–8825.